A New Class of Waveguide Dual-Mode Filters Using TM and Nonresonating Modes

Simone Bastioli, *Student Member, IEEE*, Cristiano Tomassoni, and Roberto Sorrentino, *Fellow, IEEE*

***Abstract*—An innovative class of very compact and selective waveguide dual-mode filters is presented in this paper. The basic structure is the TM dual-mode cavity. Such a cavity employs both resonant and nonresonating modes so as to provide two reflection and two transmission zeros. The high design flexibility in terms of transmission zero positioning and response bandwidth has been demonstrated by means of several single cavity designs. The design of Nth-order multiple cavity filters with N transmission zeros is presented and discussed. Different filter topologies are obtained depending on the waveguide structure used to connect adjacent cavities. An efficient mode-matching analysis method is proposed and verified for fast filter optimization. An eighth-order filter with eight transmission zeros has been designed, manufactured, and tested to demonstrate the potentialities of the filter class proposed.**

***Index Terms*—Bandpass filters, dual mode, elliptic filters, transmission zeros (TZs), waveguide filters.**

I. Introduction

In SPITE of the excellent performance in terms of loss and power handling, size and mass are well known drawbacks of waveguide-based filters. In order to alleviate such problems, dual-mode and multimode cavities exploiting multiple resonant modes within a single physical cavity have been widely employed, especially for satellite applications.

The most common dual-mode architecture is based on the circular waveguide [1] by exploiting two degenerate TE_{111} modes with orthogonal polarizations. The same concept is implemented in rectangular waveguide, where the cross section is sized so as to produce the degeneracy of the TE_{101} and TE_{011} modes [2]. Starting from these basic concepts, several dual-mode waveguide filters have been proposed in the literature [3]–[6].

The cavity volume, however, can be more efficiently used by employing TM resonant modes in combination with TE modes, thus leading to triple- and/or quadruple-mode cavities [7], [8]. Although the size reduction is significant, triple- and quadruple-mode designs are very sensitive and suffer from poor temperature stability [9].

Manuscript received June 30, 2010; revised September 16, 2010; accepted September 22, 2010. Date of publication October 28, 2010; date of current version December 10, 2010. This paper is an expanded paper from the IEEE MTT-S International Microwave Symposium, Anaheim, CA, May 23–28, 2010.

S. Bastioli and R. Sorrentino are with RF Microtech s.r.l., Perugia 06125, Italy (e-mail: bastioli@diei.unipg.it; sorrentino@rfmicrotech.com).

C. Tomassoni is with the Dipartimento di Elettronica e Informazione (DIEI), University of Perugia, Perugia 06125, Italy (e-mail: tomassoni@diei.unipg.it).

Color versions of one or more of the figures in this paper are available online at http://ieeexplore.ieee.org.

Digital Object Identifier 10.1109/TMTT.2010.2086068

Most TE dual-mode configurations proposed in the literature lead to elliptic and pseudoelliptic filter responses obtained by properly coupling the resonant modes of a single or of adjacent cavities. In any case, the number of transmission zeros is usually limited with respect to the filter order N, especially for high N.

In order to overcome such a limitation and realize even more compact dual-mode filters, a rectangular TM dual-mode cavity configuration has been proposed in [10] and [11]. Such a cavity employs both resonant and nonresonating modes so as to provide two reflection and two transmission zeros. Although the TM dual-mode cavity can be the building block for designing Nth-order filters with N transmission zeros, practical designs have been limited thus far to $N = 4$. Moreover, a clear description of the coupling and routing schemes occurring when multiple cavities are cascaded needs to be addressed.

This paper discusses in detail the properties of the TM dual-mode filter class. The design flexibility is demonstrated by means of several cavity designs along with the corresponding coupling matrix descriptions. Cavity performance parameters based on the cavity Q factor, length, and size are introduced to compare the TM dual-mode cavities with respect to the conventional $\mathrm{TE}_{101}/\mathrm{TE}_{011}$ dual-mode cavities. An efficient electromagnetic (EM) analysis method based on purely modal techniques is presented and validated. Approaches are presented for the realization of higher order filters by combining multiple TM dual-mode cavities: different filter topologies are obtained depending on the waveguide structure used to connect adjacent cavities. Finally, to show the potentialities of this class of filters, an eighth-order filter with eight transmission zeros has been designed, manufactured, and tested.

II. TM Dual-Mode Cavity

The use of nonresonating modes in combination with resonant cavity modes has been proven in [12] and [13], where single-mode cavities are arranged so as to produce one transmission zero besides the reflection zero. The TM dual-mode cavity combines the advantages of the dual-mode approach with the functionalities provided by the use of nonresonating modes.

The structure of a TM dual-mode cavity is depicted in Fig. 1. The degenerate resonant modes in the cavity are TM_{120} and TM_{210}, whose resonant frequencies are given by

$$f_{120} = \frac{c}{2\pi}\sqrt{\left(\frac{\pi}{w}\right)^2 + \left(\frac{2\pi}{h}\right)^2}$$
$$f_{210} = \frac{c}{2\pi}\sqrt{\left(\frac{2\pi}{w}\right)^2 + \left(\frac{\pi}{h}\right)^2} \quad (1)$$

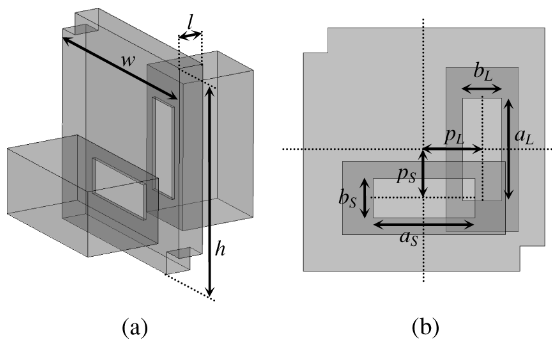

Fig. 1. TM dual-mode cavity. (a) Perspective view. (b) Front view.

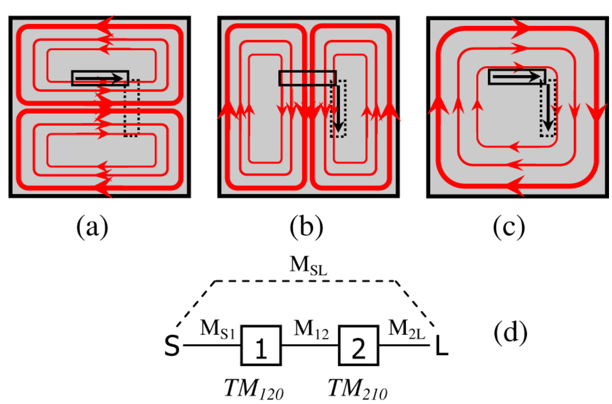

Fig. 2. Magnetic coupling. (a) Coupling between TE_{10} at input waveguide and TM_{120}. (b) coupling between TE_{10} at output waveguide and TM_{210}. (c) Coupling between TE_{10} at feeding waveguides and TM_{11}. (d) Topology.

where w and h are the cavity width and height, respectively.

Besides the TM_{120} and TM_{210} cavity modes, nonresonating modes can also be excited. The latter are waveguide modes propagating along the axial direction of the cavity, thus creating an additional input-to-output path. The nonresonating modes that are mainly involved are TM_{11} and TE_{11}.

The TM dual-mode cavity is excited by two orthogonal feeding waveguides. The coupling mechanism between the dominant TE_{10} mode of the feeding waveguides and the cavity modes is illustrated in Fig. 2: the input TE_{10} mode excites the resonant TM_{120} cavity mode, while it is uncoupled to the TM_{210} cavity mode [see Fig. 2(a)]; on the other hand, the output waveguide excites only the resonant TM_{210} cavity mode [see Fig. 2(b)]. As far as the nonresonating modes are concerned, they are coupled to both input and output waveguides [see Fig. 2(c)], thus creating a direct input-to-output coupling. Stepped corners are used within the cavity as intra-coupling discontinuities. The resulting coupling and routing scheme is shown in Fig. 2(d).

Depending on the positions p_S and p_L of the input and output waveguides, the resonant and nonresonating modes can be properly excited so as to realize either all-pole or elliptic filtering functions with a pair of real or imaginary frequency transmission zeros [11]. In the following, some design examples are reported.

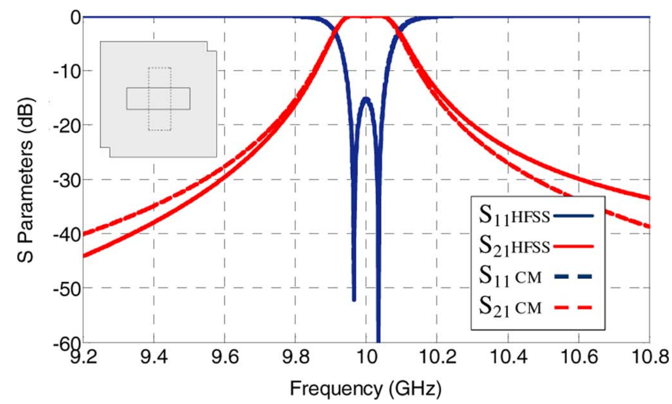

Fig. 3. HFSS simulation and coupling matrix response of a 10-GHz all-pole TM dual-mode cavity.

The first design is an all-pole TM dual-mode cavity designed at $f_0 = 10$ GHz with $\mathrm{FBW} = 1\%$ according to the following normalized coupling matrix:

$$\begin{bmatrix} 0 & 1.034 & 0 & 0 \\ 1.034 & 0 & 1.274 & 0 \\ 0 & 1.274 & 0 & 1.034 \\ 0 & 0 & 1.034 & 0 \end{bmatrix}.$$

The all-pole response can easily be obtained if the nonresonating modes are not excited. Such a situation occurs when the input and output slots are located at the center of the respective cavity wall. Fig. 3 shows the comparison between the coupling matrix response (dashed lines) and the Ansoft HFSS full-wave simulation (solid line) of the optimized structure.

The second and third examples are two elliptic TM dual-mode cavities designed at $f_0 = 10$ GHz with $\mathrm{FBW} = 1\%$, according to the following normalized coupling matrices:

$$\begin{bmatrix} 0 & 0.774 & 0 & -0.153 \\ 0.774 & 0 & 1.054 & 0 \\ 0 & 1.054 & 0 & 0.774 \\ -0.153 & 0 & 0.774 & 0 \end{bmatrix}$$

$$\begin{bmatrix} 0 & 0.914 & 0 & 0.171 \\ 0.914 & 0 & 0.934 & 0 \\ 0 & 0.934 & 0 & 0.914 \\ 0.171 & 0 & 0.914 & 0 \end{bmatrix}.$$

The former realizes two symmetric transmission zeros at $f_1 = 9.885$ GHz and $f_2 = 10.115$ GHz, while the latter generates a transmission zero pair for group delay equalization on the real axis of the complex plane. The elliptic functions are obtained when the input and output slots are properly offset with respect to the cavity center. The relative position of the input and output waveguides with respect to the stepped corners determines the sign of M_{SL}. Figs. 4 and 5 show the comparison between the coupling matrix responses (dashed lines) and the Ansoft HFSS full-wave simulation (solid line) of the optimized cavities.

Finally, in order to show the design flexibility in terms of transmission zero positioning and bandwidth, Figs. 6 and 7 show

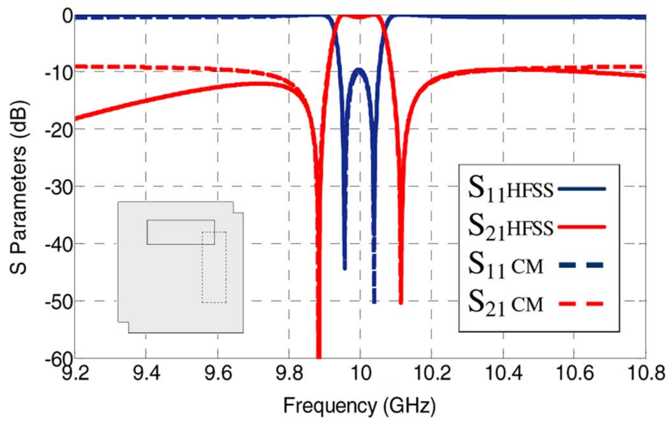

Fig. 4. HFSS simulation and coupling matrix response of a 10-GHz TM dual-mode cavity with two real frequency transmission zeros.

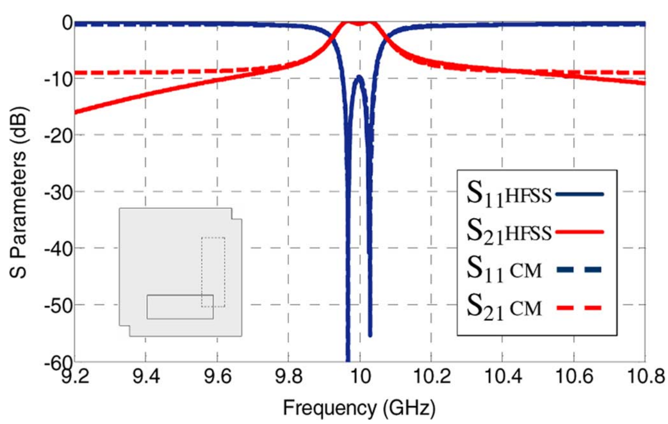

Fig. 5. HFSS simulation and coupling matrix response of a 10-GHz TM dual-mode cavity with two imaginary frequency transmission zeros.

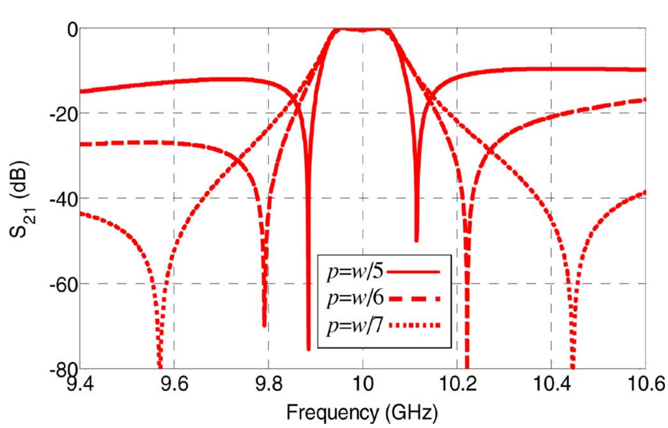

Fig. 6. HFSS simulations of elliptic TM dual-mode cavities designed with different position p for the input/output waveguides.

the full-wave simulations of some elliptic TM dual-mode cavities. Although the control is not fully independent, the position of the feeding waveguides mainly controls the transmission zero locations, while the size of the coupling slots is mainly used to modify the response bandwidth. In particular, the position $p_S = p_L = p$ allows the control of the ratio between M_{S1} and M_{SL}, while the slot dimensions $a_S = a_L = a$ and $b_S = b_L = b$ allow the increase or decrease of both M_{S1} and M_{SL}.

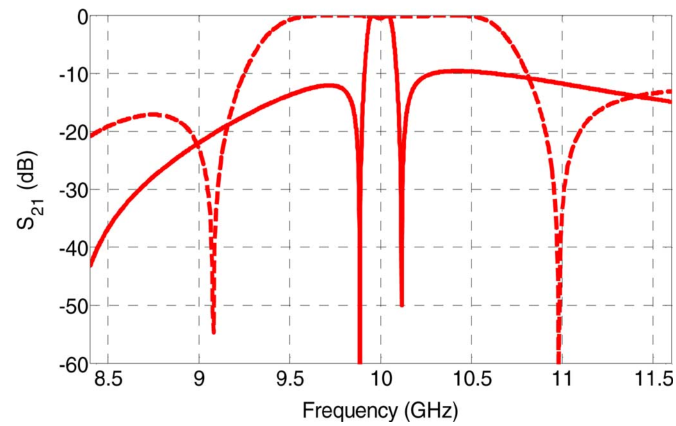

Fig. 7. HFSS simulations of two elliptic TM dual-mode cavities with relatively narrow (solid line, $a = 15$ mm and $b = 2.5$ mm) and wide (dashed line, $a = 19$ mm and $b = 5$ mm) passband.

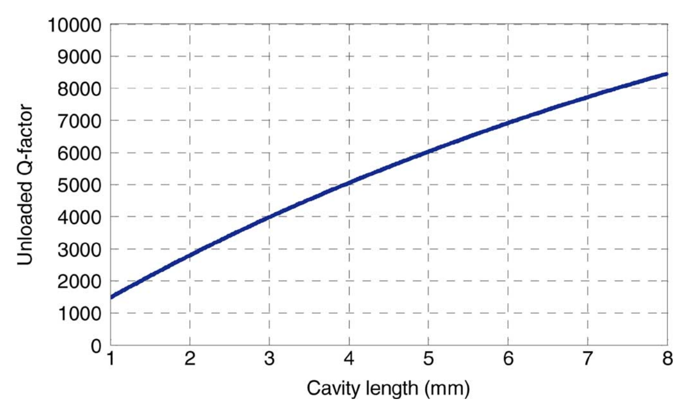

Fig. 8. Simulated unloaded Q factor versus the cavity length for a 10-GHz TM dual-mode cavity having silver surfaces.

III. Unloaded Q Factor and Cavity Size

Since the resonant TM_{120} and TM_{210} cavity modes are independent of the longitudinal direction, the cavity length l can be chosen as small as desired in order to obtain compact structures. Even for short l, the resulting unloaded Q factor is still reasonably high. Fig. 8 shows the unloaded Q factor for a 10-GHz cavity (silver surfaces, $\sigma_{\mathrm{Ag}} = 61$ MS/m) versus the cavity length. According to (1), the cavity cross section is 33.4×33.4 mm^2.

As an example, for $l = 4.5$ mm, that approximately corresponds to $\lambda_{g0}/8$, the unloaded Q factor is 5550. The resulting ratio between Q factor and volume is $Q/V = 1.10$ mm^{-3}. A conventional $\mathrm{TE}_{101}/\mathrm{TE}_{011}$ dual-mode rectangular cavity with 22.86×22.86 mm^2 cross section and 19.8 mm length has about 11190 unloaded Q factor at 10 GHz. The resulting ratio between Q factor and volume is $Q/V = 1.08$ mm^{-3}. Although the Q/V ratios are similar, the TM dual-mode cavity yields a significantly higher ratio between Q factor and cavity length (Q/l): the TM dual-mode cavity yields $Q/l = 1230$ mm^{-1}, while the $\mathrm{TE}_{101}/\mathrm{TE}_{011}$ dual-mode cavity has $Q/l = 568$ mm^{-1}.

Table I provides a complete set of performance parameters based on Q factor and size of 10-GHz TM dual-mode cavities. Regarding the Q/V ratio, if $l < 5$ mm, the TM dual-mode cavity is slightly more efficient than the $\mathrm{TE}_{101}/\mathrm{TE}_{011}$ dual-

TABLE I
Q FACTOR DATA OF10-GHz TM DUAL-MODE CAVITIES

l (mm)	Q	Q/V (mm^{-3})	Q/l (mm^{-1})
1	1480	1.33	1480
2	2800	1.25	1400
3	3970	1.18	1323
4	5060	1.13	1265
5	6030	1.08	1206
6	6925	1.03	1154
7	7738	0.99	1105
8	8486	0.95	1061

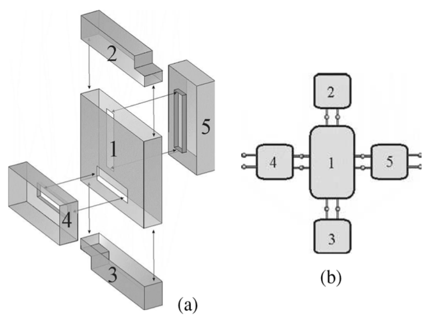

Fig. 9. (a) Structure segmentation of a TM dual-mode cavity and (b) corresponding equivalent network.

mode cavity, and *vice versa* for $l > 5$ mm. On the other hand, the Q/l ratio of a TM dual-mode cavity is considerably higher than that one of $\mathrm{TE}_{101}/\mathrm{TE}_{011}$ dual-mode cavity, independently of l. The TM dual-mode cavity offers a valuable solution whenever a moderate increase of the insertion loss can be tolerated to obtain very short filters.

IV. Mode-Matching Analysis

Although the TM dual-mode cavity has a nonseparable cross section (due to the presence of the stepped corners), a convenient and simple structure segmentation makes it possible to employ purely modal techniques.

Fig. 9(a) shows the proposed segmentation as applied to a single TM dual-mode cavity: the whole structure is segmented into five regions suitable for the application of conventional modal analyses. Regions 4 and 5, in fact, are simple steps that can be characterized by the classical in-line mode-matching technique. Similarly, regions 2 and 3 are conventional waveguide H-plane steps with the smaller port short-circuited at a certain distance. Finally, region 1 is a rectangular cavity connected through four apertures to regions 4 and 5 at the sides, and, at the top and bottom, to regions 2 and 3. The analysis of such a cavity can be carried out by using the generalized admittance matrix (GAM) approach [14]. In this manner, a multiport equivalent network is obtained for each region into which the structure has been segmented, thusobtaining the overall equivalent network of Fig. 9(b).

The proposed segmentation approach can easily be extended to multiple cavity structures, providing an efficient and accurate EM analysis suitable for fast design and optimization of complex TM dual-mode filter structures, as discussed in the following.

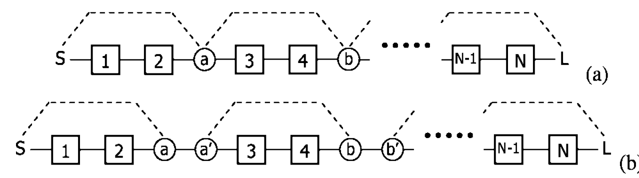

Fig. 10. Topologies of filters with second-order blocks cascaded by: (a) single or (b) multiple NRNs.

V. Filter Design Using Multiple Cavities

An all-pole TM dual-mode cavity, i.e., that not employing the nonresonating mode capability, has the same topology as a conventional $\mathrm{TE}_{101}/\mathrm{TE}_{011}$ dual-mode cavity. In this condition, multiple cavities can be coupled so as to realize direct- and/or cross-coupling as with TE dual-mode filters. A design example is reported in [11].

More interesting is the case when elliptic TM dual-mode cavities using nonresonating modes are cascaded. In this condition, the TM dual-mode cavity can be used as a second-order building block for modular design of higher order filters.

A convenient way to cascade multiple blocks is to use nonresonating nodes (NRNs) [15]. Fig. 10 shows two filter topologies using NRNs between second-order blocks [16]. In such topologies, the NRNs are shown as circles instead of square boxes. From the circuit point of view, an NRN consists of a constant shunt susceptance. Irrespective of the number of NRNs employed between adjacent blocks, both topologies yield Nth-order filtering functions with up to N transmission zeros. Each second-order block generates and completely controls its own transmission zero pair.

As done in [13] and [15], for TM single-mode cavity filters, a way to realize the nonresonating connection between adjacent cavities consists of using a relatively thick coupling slot, as illustrated in the two-cavity TM dual-mode structure of Fig. 11(a). Such a slot must be nonresonating in the vicinity of the pass-band (strongly detuned resonator), thus behaving as a constant susceptance. As long as the thickness of the coupling slot is relatively large, like e.g., a quarter wavelength, such a slot acts as a NRN with good approximation. In this condition, apart from a minor interaction due to the presence of weak spurious coupling, each cavity mainly controls its own transmission zero pair. Thick coupling slots between adjacent cavities can therefore be used to implement the topology of Fig. 10(a), having a single NRN between adjacent second-order blocks.

The nonresonating connection between adjacent cavities can also be realized using quarter-wave waveguide sections [16], as in the filter structure of Fig. 11(b). In this case, the uniform quarter-wave waveguide section is a unitary inverter, while its reference planes at the two adjacent coupling slots are NRNs. Also in this case, each cavity mainly controls its own transmission zero pair. Such a connection between adjacent cavities is suitable for the implementation of the topology of Fig. 10(b), where a pair of NRNs connected by an inverter is used between adjacent second-order blocks.

The two-cavity structure of Fig. 11(b) has been optimized to design a fourth-order bandpass filter with four transmission

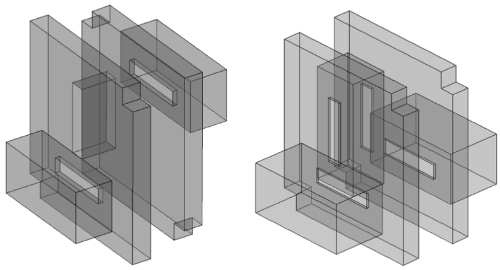

(a) (b)

Fig. 11. (a) Two-cavity TM dual-mode filters using thick coupling slot or (b) quarter-wave waveguide section between the cavities.

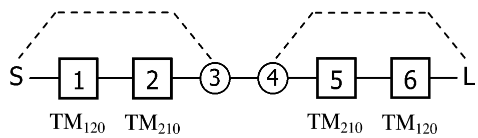

Fig. 12. Topology of a two-cavity fourth-order TM dual-mode filter using quarter-wave waveguide section.

zeros. The center frequency is 10.2 GHz with 100-MHz bandwidth. Referring to the topology of Fig. 12, the filter response is described by the normalized coupling matrix shown at the bottom of this page. The inmost coupling (M_{45}) corresponding to the quarter-wave waveguide inverter has been set to 1, considerably simplifying the filter design procedure [16]. Each cavity can first be individually designed from the corresponding submatrix, and then cascaded to the other through a quarter-wave waveguide section. The quarter-wave length has to take into account the reactive loading effects of the coupling slots. To the authors' experience, this represents a convenient starting point for the final full-wave optimization of the whole filter. Fig. 13 shows the HFSS and mode-matching simulations of the optimized structure. Observe the excellent agreement between the results. As expected, two pairs of transmission zeros yield a highly selective response.

VI. Experimental Results

A very compact and highly-selective four-cavity TM dual-mode filter has been designed and tested to prove the suitability of the proposed approach to the design of challenging filter responses. The filter center frequency is 10 GHz with 1.5% fractional bandwidth.

The structure of the optimized filter is depicted in Fig. 14(a). All cavities are designed to exploit the nonresonating mode capability

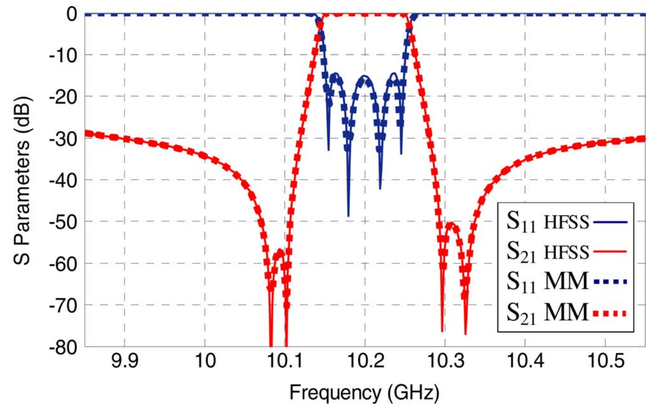

Fig. 13. HFSS and mode-matching simulations of the designed two-cavity filter with quarter-wave waveguide section [see Fig. 11(b)].

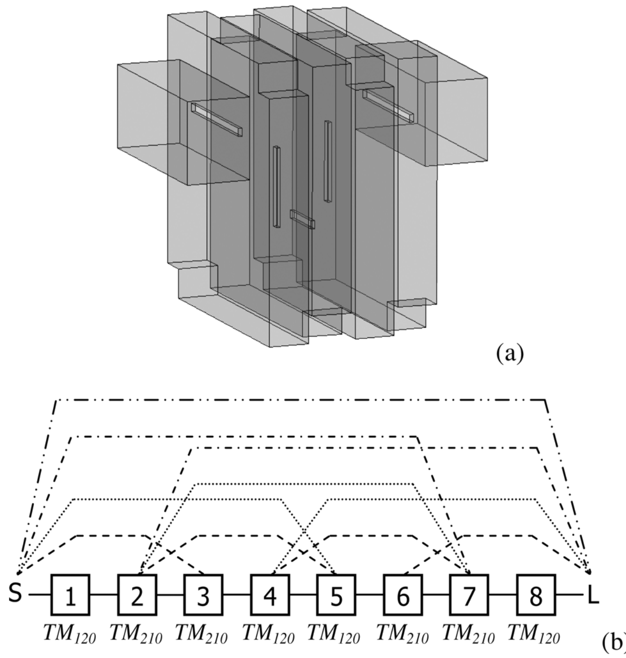

Fig. 14. Four-cavity eighth-order TM dual-mode filter with short coupling slots. (a) Filter structure. (b) Topology.

so as to generate four pairs of transmission zeros. To the best of the authors' knowledge, this is the first eighth-order dual-mode filter with eight transmission zeros without using a direct-coupling between the input and the output of the structure.

$$\begin{bmatrix} 0 & 0.892 & 0 & -0.128 & 0 & 0 & 0 & 0 \\ 0.892 & 0 & 0.825 & 0 & 0 & 0 & 0 & 0 \\ 0 & 0.825 & 0 & 0.904 & 0 & 0 & 0 & 0 \\ -0.128 & 0 & 0.904 & 0 & 1 & 0 & 0 & 0 \\ 0 & 0 & 0 & 1 & 0 & 0.588 & 0 & -0.155 \\ 0 & 0 & 0 & 0 & 0.588 & 0 & 0.884 & 0 \\ 0 & 0 & 0 & 0 & 0 & 0.884 & 0 & 0.906 \\ 0 & 0 & 0 & 0 & -0.155 & 0 & 0.906 & 0 \end{bmatrix}$$

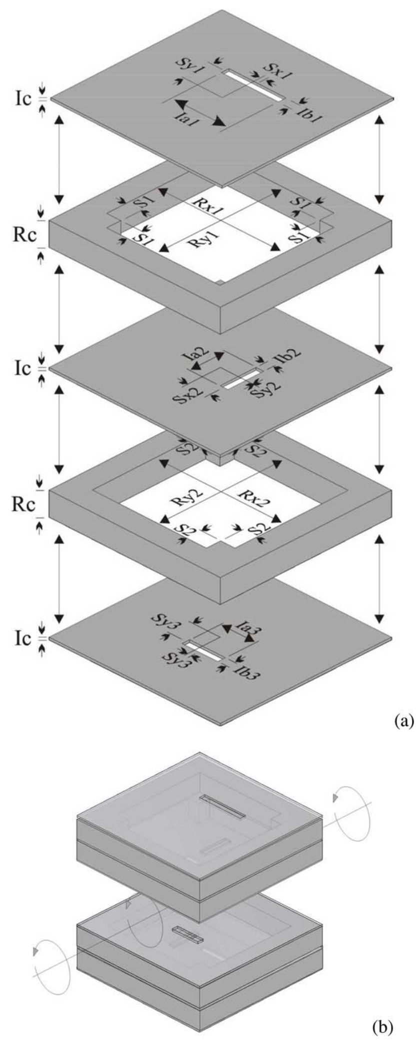

Fig. 15. Filter structure. (a) Design parameters of a filter half. (b) Symmetry between the two halves: the second half is obtained by rotating the first one around the indicated axis. WR-90 waveguides centred with respect to the first and last coupling slots constitute the filter interfaces.

The length of the cavities has been set to 5 mm: considering copper surfaces, this choice yields a 5500 unloaded Q factor. After a preliminary individual design of each cavity to properly locate resonances and transmission zeros, the cavities have been first cascaded together by means of relatively thick coupling slots, as illustrated in Section V. The efficient EM analysis technique described in Section IV has then been used for a fast full-wave optimization of the whole filter. As is apparent in the final structure of Fig. 14(a), during the filter optimization, the thicknesses of the coupling slots between adjacent cavities have been forced to be very short (0.5 mm) so as to obtain a very compact filter.

If the thickness of the coupling slots is small, strong spurious coupling phenomena occur within the filter. This is due to the nonresonating modes that propagate through the cavities and the slots along the filter. As a result, multiple cross-coupling coefficients occur among the input/output and the cavity resonant modes. In this condition, the inner coupling slots are not conveniently described by the NRN model anymore, and simple inverters can be used. Similar phenomena have been observed in [17] for TM single-mode filters.

TABLE II
FILTER DIMENSIONS

Parameter	Value (mm)	Parameter	Value (mm)
Ia1	15	*Ib1*	2
Sx1	0.25	*Sy1*	7.26
Ia2	9.4	*Ib2*	2
Sx2	5.711	*Sy2*	0.0
Ia3	9.4	*Ib3*	2
Sx3	0.4	*Sy3*	5.7426
Rx1	33.543	*Ry1*	33.7416
Rx2	33.5246	*Ry2*	33.5039
S1	3.7547	*S2*	3.3174
Rc	5	*Ic*	0.5

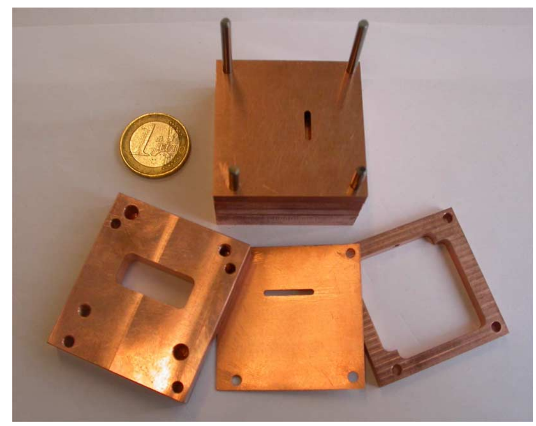

Fig. 16. Disassembled prototype of the four-cavity TM dual-mode filter.

The designed filter with short coupling slots can be properly described by the coupling scheme in Fig. 14(b). Such a cross-coupled topology can realize eighth-order filtering functions with eight transmission zeros as the eighth-order version of the topologies of Fig. 10. It can easily be demonstrated that the coupling coefficients of the cross-coupled topology can be directly calculated from those of Fig. 10(b) when the NRN susceptances are zero. In contrast with the latter, however, in the cross-coupled topology the four transmission zero pairs are not independently controlled by the individual cavities anymore: the whole set of coupling and cross-coupling determines the position of the transmission zeros.

The coupling matrix implementing the response of the designed filter is shown in the equation at the bottom of the following page. All cross-coupling mechanisms are ascribed to nonresonating modes that bypass single and/or multiple cavities. As an example, M_{S5} is due to the nonresonating modes that bypass the first and the second cavities making a coupling between the fundamental TE_{10} at the input and the TM_{120} cavity mode in the third cavity. Since the cross-coupling magnitude decreases with the number of bypassed cavities and slots, prescribed relationships between some of the coupling coefficients must be expected: as an example, $|M_{S3}| > |M_{S5}| > |M_{S7}| > |M_{SL}|$. Moreover, due to the positioning of the coupling slots, some cross-coupling mechanisms are not present in the structure: in particular, the resonant cavity mode having magnetic field direction perpendicular with respect to a coupling

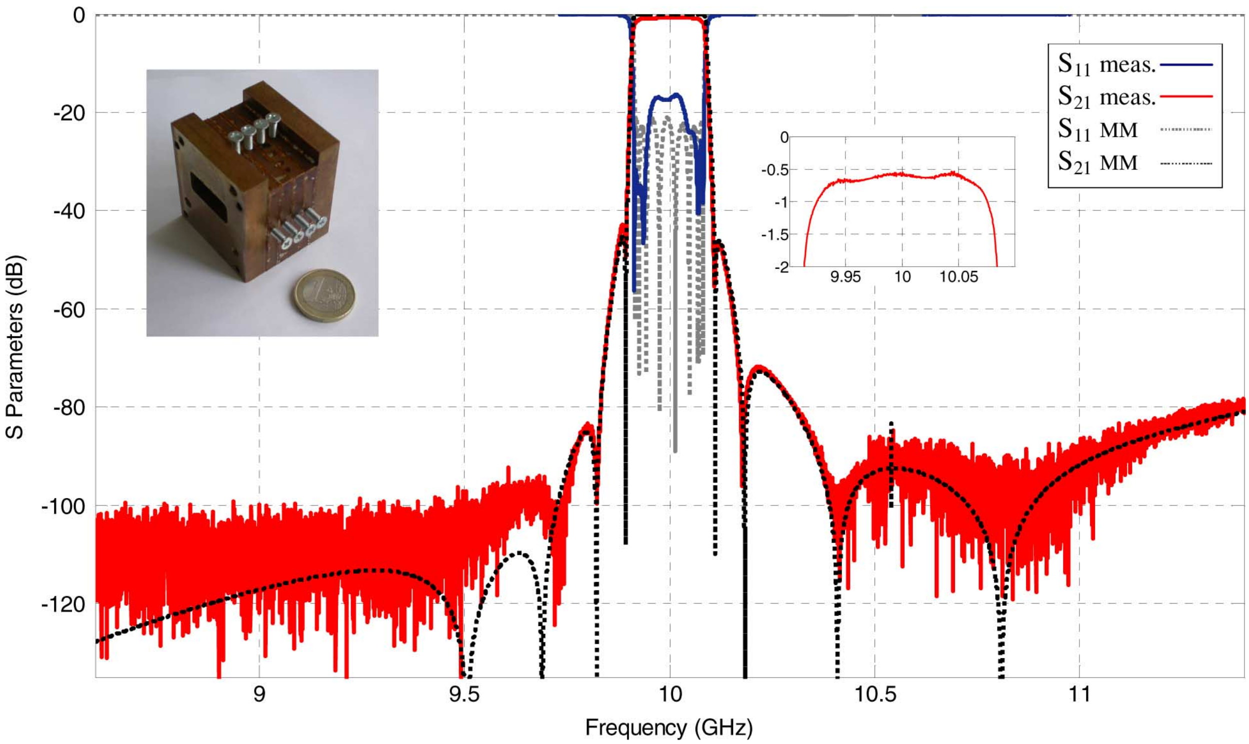

Fig. 17. Measurement and mode-matching simulation of the four-cavity TM dual-mode filter (inset, assembled prototype).

slot will not be excited by the nonresonating modes coming from that slot. As an example, although the TM_{210} cavity mode in the second cavity can be excited by the nonresonating modes coming from the filter input (M_{S3}), it cannot be excited by the nonresonating modes coming from the output ($M_{35} = M_{36} = M_{37} = M_{38} = M_{3L} = 0$).

Since the transmission zero pairs are not independently controlled, more effort is required for the design and full-wave optimization of a filter with short coupling slots. This fact further highlights the importance of using efficient EM analysis techniques. To give an idea, the mode-matching based technique described in Section IV takes only 41 s for an accurate simulation of the eighth-order filter (HFSS takes about 25 min). According to the coupling matrix, in the optimized structure, the first and the second cavities, along with their slots, are equal to the fourth and third cavities, respectively. With reference to Fig. 15, Table II quotes all the filter dimensions.

The filter has been manufactured by machining several copper layers, as shown in Fig. 16. Thicker layers (5 mm) constitute the cavities of the filter, while thinner layers (0.5 mm) contain the coupling slots. The layers have then been soldered together. The assembled prototype is shown in the inset of Fig. 17. Apart from the feeding waveguide flanges (standard WR-90 interface), the filter length is 22 mm, that approximately corresponds to one-half of the guided wavelength.

The measurements of the prototype are shown in Fig. 17, along with the corresponding mode-matching simulation. The agreement between the two has been obtained after a little tuning involving only the cavity resonant frequencies: to this purpose, a pair of orthogonal screws has been inserted into each cavity. Since the screws are located at the maxima of the magnetic field, the resonant frequencies increase with the screw penetration. Thanks to the eight transmission zeros, the filter response is highly selective and provides at the same time a

$$\begin{bmatrix}
0 & 1.05 & 0 & -0.0386 & 0 & 0.022 & 0 & -0.378m & 0 & 0.02371m \\
1.05 & 0 & 0.894 & 0 & 0 & 0 & 0 & 0 & 0 & 0 \\
0 & 0.894 & 0 & 0.57 & 0 & -0.09 & 0 & 0.597m & 0 & -0.378m \\
-0.0386 & 0 & 0.57 & 0 & 0.642 & 0 & 0 & 0 & 0 & 0 \\
0 & 0 & 0 & 0.642 & 0 & 0.535 & 0 & -0.09 & 0 & 0.022 \\
0.022 & 0 & -0.09 & 0 & 0.535 & 0 & 0.642 & 0 & 0 & 0 \\
0 & 0 & 0 & 0 & 0 & 0.642 & 0 & 0.57 & 0 & -0.0386 \\
-0.378m & 0 & 0.597m & 0 & -0.09 & 0 & 0.57 & 0 & 0.894 & 0 \\
0 & 0 & 0 & 0 & 0 & 0 & 0 & 0.894 & 0 & 1.05 \\
0.02371m & 0 & -0.378m & 0 & 0.022 & 0 & -0.0386 & 0 & 1.05 & 0
\end{bmatrix}$$

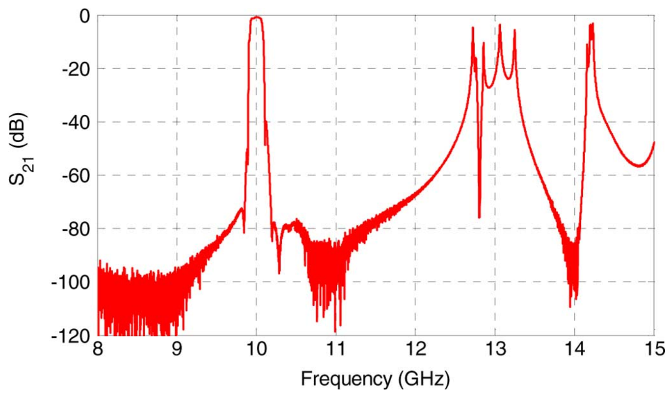

Fig. 18. Broadband measurement of the four-cavity TM dual-mode filter.

high out-of-band rejection. The measured return loss is better than 16 dB, while the insertion loss is 0.6 dB (inset of Fig. 17). The actual unloaded Q factor is estimated to be about 4500. Observe that the return loss at the center of the passband is slightly lower than expected. This is mainly due to the fact that the tuning screws actually alter the intra-coupling between resonant cavity modes. The introduction of screws located at 45° (within the stepped corners) would enhance the tuning capability and solve such a problem. A more complete tuning capability would be obtained by inserting additional screws or discontinuities at the input and output of the filter, as well as into the inner coupling slots. Anyway, since the inner coupling slots are realized within very thin metallic sheets, high precision manufacturing processes could be adopted with moderate costs. This would avoid the tuning of the inner coupling slots.

Fig. 18 shows a broadband response demonstrating a spurious-free stopband extending up to 12.6 GHz. Such a performance is comparable with that of some TE dual-mode filters [6]. The spurious responses can mainly be ascribed to the resonances occurring within the coupling slots, as well as to the higher order TM_{220} mode. It must be pointed out that if the nonresonating modes are partially or not exploited (i.e., not all the available transmission zero pairs are generated), the spurious performance of a TM dual-mode filter can be significantly improved.

VII. Conclusion

The TM dual-mode filter class allows the realization of very compact and highly selective waveguide filters. The TM dual-mode cavity is itself an elliptic response structure able to generate two transmission zeros besides the two poles. In contrast with conventional TE dual-mode filters, Nth-order filters with N transmission zeros can be realized, being at the same time very compact along the longitudinal direction. By a proper structure segmentation, an efficient mode-matching analysis can be used for fast filter design and optimization. Multiple cavity configurations have been designed and discussed. Depending on the waveguide structure used as interconnecting section between adjacent cavities, such as thick or thin coupling slots and quarter-wave waveguide sections, different topologies must be used to properly describe the filter structure.

The filter class has been experimentally validated by a 10-GHz four-cavity eighth-order filter with eight transmission zeros. Besides generating the maximum allowable number of transmission zeros, the overall length of the filter is just one half of the guided-wavelength.

References

[1] A. E. Williams, "A four-cavity elliptic waveguide filter," *IEEE Trans. Microw. Theory Tech.*, vol. MTT-18, no. 12, pp. 1109–1114, Dec. 1970.

[2] A. E. Atia and A. E. Williams, "New types of waveguide bandpass filters for satellite transponders," *COMSAT Tech. Rev.*, vol. 1, no. 1, Fall, 1971.

[3] R. V. Snyder, "Multicavity dual mode filter," U.S. Patent 3936775, Sep. 30, 1974.

[4] X. P. Liang, K. A. Zaki, and A. E. Atia, "Dual-mode coupling by square corner cut in resonators and filters," *IEEE Trans. Microw. Theory Tech.*, vol. 40, no. 12, pp. 2294–2302, Dec. 1992.

[5] V. Boria, M. Guglielmi, and P. Arcioni, "Accurate CAD for dual-mode filters in circular waveguide including tuning elements," in *IEEE MTT-S Int. Microw. Symp. Dig.*, 1997, pp. 1575–1578.

[6] M. Guglielmi, P. Jarry, E. Keherve, O. Roquebrun, and D. Schmitt, "A new family of all-inductive dual-mode filters," *IEEE Trans. Microw. Theory Tech.*, vol. 49, no. 10, pp. 1764–1769, Oct. 2001.

[7] W. C. Tang and S. K. Chaudhuri, "A true elliptic function filter using triple mode degenerate cavities," *IEEE Trans. Microw. Theory Tech.*, vol. MTT-34, no. 11, pp. 1449–1454, Nov. 1984.

[8] R. Bonetti and A. Williams, "Application of dual TM modes to triple- and quadruple-mode filters," *IEEE Trans. Microw. Theory Tech.*, vol. MTT-35, no. 12, pp. 1143–1149, Dec. 1987.

[9] I. C. Hunter, L. Billonet, B. Jarry, and P. Guillon, "Microwave filters—Applications and technology," *IEEE Trans. Microw. Theory Tech.*, vol. 50, no. 3, pp. 794–805, Mar. 2002.

[10] S. Bastioli, L. Marcaccioli, C. Tomassoni, and R. Sorrentino, "Ultra-compact highly-selective dual-mode pseudoelliptic filters," *IET Electron. Lett.*, vol. 46, no. 2, pp. 147–149, Jan. 2010.

[11] S. Bastioli, L. Marcaccioli, and R. Sorrentino, "TM dual-mode pseudoelliptic filters using nonresonating modes," in *IEEE MTT-S Int. Microw. Symp. Dig.*, Anaheim, CA, May 2010, pp. 880–883.

[12] S. Amari and U. Rosenberg, "Characteristics of cross (by-pass) coupling through higher/lower order modes and their applications in elliptic filter design," *IEEE Trans. Microw. Theory Tech.*, vol. 53, no. 10, pp. 3135–3141, Oct. 2005.

[13] U. Rosenberg, S. Amari, and J. Bornemann, "Inline TM_{110} -mode filters with high design flexibility by utilizing bypass couplings of nonresonating $\mathrm{TE}_{10/01}$ modes," *IEEE Trans. Microw. Theory Tech.*, vol. 51, no. 6, pp. 1735–1742, Jun. 2003.

[14] G. Conciauro, M. Guglielmi, and R. Sorrentino, *Advanced Modal Analysis*. New York: Wiley, 2000.

[15] S. Amari, U. Rosenberg, and J. Bornemann, "Singlets, cascaded singlets and the nonresonating node model for modular design of advanced microwave filters," *IEEE Microw. Wireless Compon. Lett.*, vol. 14, no. 5, pp. 237–239, May 2004.

[16] S. Amari and U. Rosenberg, "New building blocks for modular design of elliptic and self-equalized filters," *IEEE Trans. Microw. Theory Tech.*, vol. 52, no. 2, pp. 721–736, Feb. 2004.

[17] S. Amari, U. Rosenberg, and J. Bornemann, "Adaptive synthesis and design of resonator filters with source/load-multiresonator coupling," *IEEE Trans. Microw. Theory Tech.*, vol. 50, no. 8, pp. 1969–1978, Aug. 2002.

Simone Bastioli (S'10) was born in Spoleto, Italy, on June 19, 1981. He received the Master degree (with honors) in electronic engineering and Ph.D. degree in electronic engineering from the University of Perugia, Perugia, Italy, in 2006 and 2010, respectively.

In 2005, he was an Intern with Ericsson AB, Mölndal, Sweden, where he was involved with the design of waveguide filters and transitions for microwave applications. In 2009, he carried out a portion of his doctoral research with RS Microwave Inc., Butler, NJ. In 2010, he joined RF Microtech s.r., Perugia, Italy (a spin-off of the University of Perugia), where he is currently a Microwave Designer and Researcher. His research activities include the design of microwave filters and diplexers, as well as low-temperature co-fired ceramic (LTCC) and reconfigurable circuits.

Dr. Bastioli is a member of the IEEE Microwave Theory and Techniques Society (IEEE MTT-S) and a member of the European Microwave Association (EuMA). In 2008, he was the recipient of the Best Student Paper Award (First Place) presetned at the IEEE MTT-S International Microwave Symposium (IMS), Atlanta, GA. In 2008, he was also the recipient of the Young Engineers Prize presented at the European Microwave Conference, Amsterdam, The Netherlands. In 2009, he was the recipient of the Hal Sobol Travel Grant presented at the IEEE MTT-S IMS, Boston, MA. In 2010, he was a finalist at the Student Paper Competition of the IEEE MTT-S IMS, Anaheim, CA.

Cristiano Tomassoni was born in Spoleto, Italy, in 1969. He received the Laurea degree and Ph.D. degree in electronics engineering from the University of Perugia, Perugia, Italy, in 1996 and 1999, respectively.

In 1999, he was a Visiting Scientist with the Lehrstuhl für Hochfrequenztechnik, Technical University of Munich, Munich, Germany. In 2001, he was a Guest Professor with the Fakultät für Elektrotechnik und Informationstechnik, Otto-von-Guericke University, Magdeburg, Germany. He is currently an Assistant Professor with the University of Perugia. His main area of research is the modeling and design of waveguide devices and antennas. His research interests also include the development of hybrid methods for the design of microwave components.

Roberto Sorrentino (M'77–SM'84–F'90) received the Doctor degree in electronic engineering from the University of Rome "La Sapienza," Rome, Italy, in 1971.

In 1974, he became an Assistant Professor of microwaves with the University of Rome "La Sapienza." He was an Adjunct Professor with the University of Catania, the University of Ancona, and the University of Rome "La Sapienza" (1977–1982), where he then was an Associate Professor from 1982 to 1986. In 1983 and 1986, he was a Research Fellow with The University of Texas at Austin. From 1986 to 1990, he was a Professor with the University of Rome "Tor Vergata." Since November 1990, he has been a Professor with University of Perugia, Perugia, Italy, where he was the Chairman of the Electronic Department, Director of the Computer Center (1990–1995), and Dean of the Faculty of Engineering (1995–2001). In 2007, he founded RF Microtech s.r.l., Perugia, Italy (a spinoff of the University of Perugia). He has authored or coauthored over 100 technical papers in international journals and 200 refereed conference papers. He edited a book for the IEEE Press and coauthored three books on advanced modal analysis (2000), microwave filters (2007), and RF and microwave engineering (2010). His research activities have been concerned with various technical subjects such as the EM wave propagation in anisotropic media, the interaction of EM fields with biological tissues, but mainly with numerical methods and computer-aided design (CAD) techniques for passive microwave structures, and the analysis and design of microwave and millimeter-wave circuits. In recent years, he has been involved in the modeling and design of RF microelectromechanical systems (RF-MEMS) and their applications on tunable and reconfigurable circuits and antennas.

Dr. Sorrentino was the International Union of Radio Science (URSI) vice chair (1993–1996) and chair (1996–1999) of Commission D (Electronics and Photonics). Since 2007, he has been the president of the Italian Delegation of URSI. In 1998, he was one of the founders of the European Microwave Association (EuMA) and was its President from its constitution until 2009. In 2002, he was among the founders and first president of the Italian Electromagnetic Society (SIEm), which he chaired until 2008. From 1998 to 2005, he was a member of the High Technical Council, Italian Ministry of Communications. From January 1995 to April 1998, he was the editor-in-chief of the IEEE MICROWAVE AND GUIDED WAVE LETTERS. From 1998 to 2005, he was on the Administrative Committee of the IEEE Microwave Theory and Techniques Society (IEEE MTT-S). He is a member of Technical Committees MTT-15 on Field Theory and MTT-1 on Computer-Aided Design. In 1993, he was the recipient of the IEEE MTT-S Meritorious Service Award. In 2000, he was one of the recipients of the IEEE Third Millennium Medal. In 2004, he was the recipient of the Distinguished Educator Award of the IEEE MTT-S.